

Surface patterning on indium phosphide with low energy Ar atoms bombardment: an evolution from nanodots to nanoripples

Indra Sulania^{1*}, Ambuj Tripathi¹, D. Kabiraj¹, Matthieu Lequeux² and Devesh Avasthi¹

¹Inter University Accelerator Centre, New Delhi 110067, India

²National Institute of Polytechnique, Grenoble 38016, France

*Corresponding author. Tel.: (+91) 11 26893955, 268992603; Fax: (+91) 11 26893666; E-mail: indra@iuac.res.in

Received: 31 May 2010, Revised: 15 July 2010 and Accepted: 20 July 2010

ABSTRACT

In the present study, Indium Phosphide (InP) (100) samples with a thickness of ~ 0.5 mm have been bombarded with 1.5 keV Argon atoms for a fixed fluence of 8×10^{16} atoms/cm². The angle of incidence of the atom beam has been varied from normal incidence to 76° with respect to surface normal. The bombarded surface shows the nanostructures as analysed by Atomic Force Microscopy (AFM). For normal and near normal incident angles of the beam, nanodots pattern have been observed and after a critical angle of incidence, the dots begin to align and with further increase of angle, nanostructures elongate along the beam direction. At 63° incidence, a well ordered ripple pattern has been reported. The evolution of nanostructures from nanodots to nanoripples has been analysed in terms of their size, shape and roughness by means of AFM imaging. Copyright © 2010 VBRI press.

Keywords: Atom beam sputtering; nano-dots; nano-ripples; AFM.



Indra Sulania is working as Scientist at IUAC, New Delhi, India. She is mainly working on Scanning Probe Microscope facility. Her area of research interest is the investigations of nanostructures formation on various materials and thin films using low energy ion beams. These nanostructures include the nanoripples, nanodots, nanoholes etc.



D. Kabiraj is working as Scientist at IUAC, India. He did his Ph.D. from Jawaharlal Nehru University, New Delhi. He is the In-charge of Thin Film and Target Development Laboratory. He has research interest on optical and transport properties of semiconductors and their modifications by high energy light ions irradiation. His research focuses on ion beam interaction with composite thin films to form nano-alloy and growth of rare-earth doped thin film of wide band gap materials etc.



Ambuj Tripathi is Scientist at Inter University Accelerator Centre (IUAC), New Delhi. He is in charge of materials science (online experimental facilities) and SPM Lab at IUAC. His main areas of research are (1) Ion beam modification of surfaces and (2) Ion beam induced synthesis and modification of nanoparticles. He has played a key role in the setting up of the experimental beam line and *in-situ* facilities such as *in-situ* XRD, *in-situ* UHV STM, *in-situ* QMA set up. He did his Ph.D. from University of

Allahabad in 2006 on the Study of Irradiation Effects on Surfaces



Matthieu Lequex was born in 1983 in Paris. In 2007, he obtained a triple Master Degree in Microelectronics from the Ecole Polytechnique Fédérale de Lausanne, the Politecnico di Torino and the Institut National Polytechnique de Grenoble. Before completing his academic career, he did an internship as Research and development engineer at the R&D center of Soitec in Grenoble to develop a Smart Cut process.



D.K. Avasthi is working as Scientist at IUAC, New Delhi. He is the present group leader for materials Science Group and radiation biology group at IUAC, New Delhi. He has keen interest on in situ/online measurements during ion irradiation like (i) Electronic sputtering by on-line ERDA (ii) Phase transformation and growth/reduction of nanoparticle size by in-situ XRD, (iii) on-line Measurement of gas release during ion

irradiation (iv) In-situ raman spectrometer (being setup) Established role of thermal spike in SHI induced mixing in metal/Si and metal/metal systems. Synthesis and engineering of nanostructures by ion beams, ion beam interaction with nanodimensional systems, Synthesis of metal nanoparticles embedded in different matrices by atom beam co-sputtering and understanding of the same by simulation, Creation of functional surfaces by ion beams.

Introduction

Due to an increasing demand of devices in micrometric and nanometric dimensions in IC industry, further miniaturization of circuits is needed. The lithography methods are used to produce small dimension nanostructures such as quantum dots and quantum wires but lithography is limited in resolution ~ 50 nm [1]. Therefore, it is of interest to explore other methods to produce even smaller nano scale surfaces features. One of such method is the ion bombardment-induced surface modification. There are extensive evidences that depending on the experimental conditions, ion bombardment can result in ordered structures in nano dimensions on variety of materials [2-7]. This technology has generated a lot of experimental and theoretical interest in recent years. The evolution of nanostructures induced by ion bombardment was first explained by Bradley and Harper with a linear equation (1) [8]:

$$\frac{\partial h}{\partial t} = -v_0 + \nu \nabla^2 h - D_{\text{eff}} \nabla^4 h \quad \text{----- (1)}$$

Where, v_0 is the constant erosion velocity of the plane surface, and ν is the effective surface tension which is caused by the erosion process and usually has a negative value leading to a surface instability. D_{eff} is the surface diffusion coefficient, which is the sum of thermal diffusion and ion-induced diffusion. Surface evolution is caused due to interplay between sputtering induced roughening and diffusion induced smoothing. With the development of SPM technique such as STM and AFM, many studies have quantified the bombarded surface topography. Researchers have concentrated themselves on one or more experimental parameter during ion bombardment such as temperature of the substrate, angle of incidence of the ion beam, fluence (bombardment time), ion current density, ion energy, nature of the bombarding ion as well as of host material. Another parameter is the crystal orientation but it seems that the most studied orientation is (100) orientation. Sung et al. [9] bombarded InP (001) with 5 eV to 500 eV Ar^+ ions at temperatures varying from room temperature up to 600°C and concluded that an ion energy threshold of 40 eV was required for the surface roughening to begin and to create Indium-rich clusters and islands. Demanet et al. [10] studied the dependence of topographic changes on InP (100) with dose density using 0.5 keV Ar^+ ion and 5 keV

Kr^+ ions at a lower current density of $8 \mu\text{A}/\text{cm}^2$ and found out the wavelength dependence on the dose density as $\lambda \sim \phi^{0.2}$. Recent works [11, 12] have also studied scaling behaviour of bombarded surfaces according to scaling theory of sputtered surface [13, 14] by determining the roughness and the growth exponent and also showed that the nanostructures obtained are Indium rich due to preferential sputtering of Phosphorus. Frost et al. [15] studied the dependence of nanodots pattern on InP (100) with angle of incidence of ion beam. The authors have used 500 eV Ar^+ ions with a high ion flux of $150 \mu\text{A}/\text{cm}^2$ and rotating sample. A well ordered hexagonal pattern of nanodots is formed when the angle of incidence compared to sample normal is kept under 50° beyond which, the periodic pattern is lost.

However, in the above mentioned studies, the variation in the incidence angle parameter has not been extensively studied for InP, especially for such a large range, even though it is shown that choosing different angles of bombardment, yields to different surface nanostructuring pattern. In the present work, we discuss the formation of structures obtained in terms of their variation in shapes, sizes, height, roughness etc. through topographic studies with the help of AFM imaging and try to find out the possible reason for such a behavior towards the incidence angle of the beam.

Experimental

In the present experiment, 1.5 keV Argon (Ar) atoms were used to bombard the commercially available samples of Fe-doped semi-insulating Indium Phosphide (InP) (100) from wafertech Inc. U.K., at 300 °K. The base pressure of the chamber was around 5×10^{-6} mbar and 3×10^{-3} mbar during bombardment. An atom dose of 8×10^{16} atoms/ cm^2 was used (corresponding to a bombardment time of 15 minutes at a flux of $15 \mu\text{A}/\text{cm}^2$) for the experiment. The angle of incidence of the atom beam was changed from normal to 76° incidence for these angles, $\theta_{\text{atom}} = 0^\circ, 7^\circ, 13^\circ, 23^\circ, 38^\circ, 45^\circ, 52^\circ, 63^\circ$ and 76° .

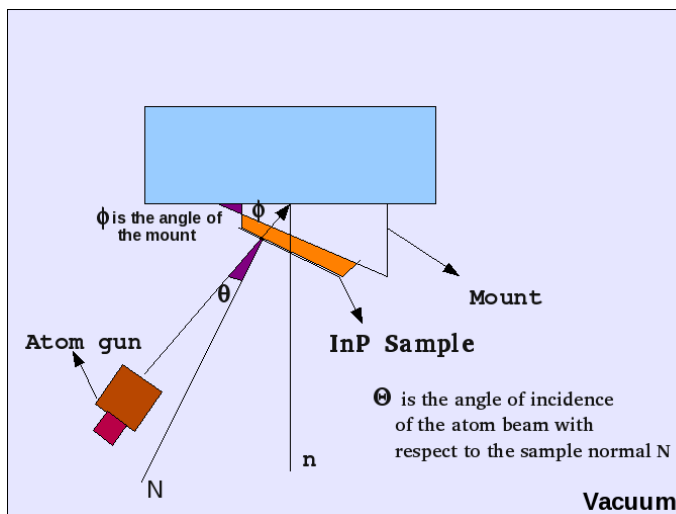


Fig. 1. Schematic of the sample and mount placed inside the sputtering chamber.

Fig. 1 shows the schematic of the set up of sputtering unit designed indigenously at IUAC, New Delhi [16-20]. It has an Ar source, which delivers Ar atoms with a current density of $30 \mu\text{A}/\text{cm}^2$. The samples were mounted at the top part of the chamber as shown in the **Fig. 1**. The atom gun is fixed at 45° with respect to the sample normal. Different Aluminium mounts were fabricated for the samples to achieve different angle of incidences. The samples were placed on these mounts. Changing the mount changed the angle of the atom beam incidence on the target. The atom beam modified morphology of the samples were studied using Multi-mode Nanoscope IIIa Atomic Force Microscopy (AFM). The measurements were performed in air in the Tapping Mode using Silicon Nitride tips from Veeco (Model RTESP, Wafer 1144). The apex of the tip has a radius of curvature of ~ 10 nm. The corresponding two dimensional auto-correlation functions for surface areas of $1 \mu\text{m} \times 1 \mu\text{m}$ have also been taken from AFM. The two-dimensional auto-correlation function is given by the relation (2):

$$C(\vec{r}, t) = \langle h(\vec{r}, t) h(\mathbf{0}, t) \rangle \quad (2)$$

Where, $h(\vec{r}, t)$ is the height at point $\vec{r}(x, y)$ at time t and $h(\mathbf{0}, t)$ is the reference point with respect to which correlation is taken. The auto-correlation function shows the spatial symmetry/ordering of the structures obtained on the bombarded InP surface.

Results

The morphological evolution of the different nanostructures obtained on the surface of InP (100) with the variation in angle of incidence parameter was extracted using AFM as shown in **Fig. 2**. The AFM image of the pristine sample is shown in **Fig. 2A**. The surface observed is flat and featureless with root mean square (rms) roughness ~ 0.2 nm. On bombarding with 1.5 keV Ar atoms at an angle of 0° with respect to the surface normal, nanodots pattern was evolved on the surface of InP (100). The pattern is clearly seen in the AFM image given in **Fig. 2B**. The average diameter of nanodots was found to be 67 ± 7 nm (as seen with the line profile in AFM images) with an average height of 21.3 nm. The rms roughness was found to be 8.3 nm. The inset of the image shows the auto-correlation of the AFM image, which represents the spatial ordering of the nanodots in square symmetry (a central dot surrounded by a square). As the angle was increased to 7° (**Fig. 2C**), nanodots were observed with an improvement in their lateral ordering. The mean diameter of nanodots was found to be 114 ± 16 nm with an average height of 9.5 nm. The rms roughness was found to be 4.7 nm. At 13° incidence, nanodots pattern (**Fig. 2D**) visible with smaller size $\sim 32 \pm 5$ nm and height ~ 4.0 nm, compared to previous two angles. The auto-correlation image shows that spatial ordering of the nanodots has improved to hexagonal symmetry (a central dot surrounded by a hexagon). The rms roughness was around 1.2 nm. At 23° incidence, the nanodots align in the beam direction (**Fig. 2E**). The average diameter of nanodots was found to 46 ± 7 nm with average height of 4.2 nm. At 38° incidence, elongation of the nanodots was observed along the beam direction with

wavelength of the elongated structures ~ 40 nm (**Fig. 2F**). The height of the structures was ~ 5 nm. The inset shows that there is ordering along one direction. At 45° incidence, the alignment of nanodots was observed (**Fig. 2G**) along the beam direction with a periodicity of ~ 45 nm and rms roughness ~ 1.3 nm. Structures observed at 53° (**Fig. 2H**) were similar to 45° except that dots were more elongated with a roughness of 1.8 nm and periodicity ~ 55 nm. There is formation of nanoripples at incidence of 63° (**Fig. 2I**) with wavelength ~ 60 nm and height ~ 4 nm. The auto-correlation image shows a well-ordered nanoripple formation along the beam direction. Finally, for 76° , no significant features were visible and roughness of surface was almost equal to that of pristine sample.

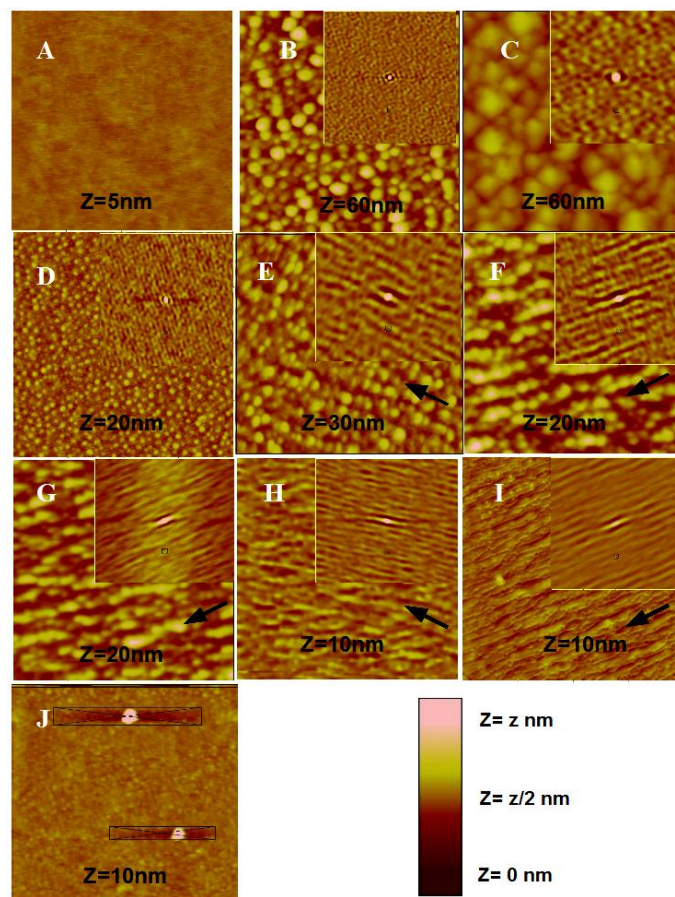


Fig. 2. AFM micrograph ($1 \mu\text{m} \times 1 \mu\text{m}$) of the pristine InP (100) and bombarded samples at different angles of incidences. Inset shows the corresponding auto-Correlation images. From A to J, Pristine and bombarded samples at $\theta_{\text{atom}} = 0^\circ, 7^\circ, 13^\circ, 23^\circ, 38^\circ, 45^\circ, 52^\circ, 63^\circ$ and 76° respectively.

Discussion

We can categorise our results into three main parts: (i) Dot formation (at $\theta_{\text{atom}} = 7^\circ, 13^\circ, 23^\circ$), (ii) the transition from dots to ripples (at $\theta_{\text{atom}} = 31^\circ, 38^\circ$ and 45°) and (iii) the ripple formation (at $\theta_{\text{atom}} = 53^\circ$ and 63°). For normal and near normal ($\theta_{\text{atom}} = 7^\circ, 13^\circ, 23^\circ$) incidences, nanodots pattern is observed, formation of these dots is due to the dominating erosion term in the BH equation which makes the surface rough as observed at 0° incidence. At these

incident angles the component of the force of the incoming beam along the perpendicular direction (horizontal plane) is zero, the only contribution is in the direction of the beam (vertical plane). Due to this component, the energy is equally distributed through collision cascades around the ion path with Gaussian distribution. This leads to sputtering of material from the surface that makes the surface rough. Few reports on InP have shown [9, 11-14] that the structures are rich in In. InP is III-V compound semiconductor. On bombardment with energetic Ar atoms, the P atoms in InP are sputtered preferentially as the mass of Ar is close to the mass of P and hence the surface is rich in In [11, 12]. At 13° incidence, the best morphology is observed in terms of the uniformity in the size of dots. The nanodots observed at 13° incidence are smaller in size and well ordered too as compared to the previous two angles (Fig. 3).

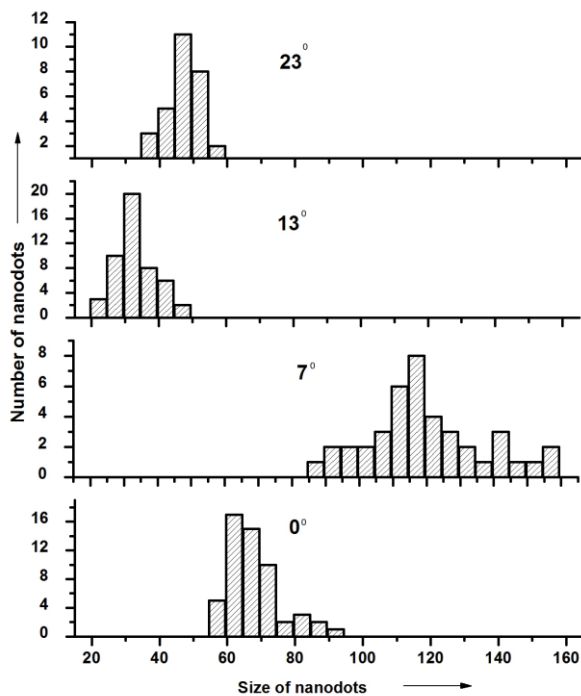


Fig. 3. Size distribution of the nanodots for $\theta_{\text{atom}} = 0^\circ, 7^\circ, 13^\circ, 23^\circ$.

At $\theta_{\text{atom}} = 31^\circ, 38^\circ$ and 45° incidence, transition from nanodots to nanoripples is observed due to elongation of dots. The elongation of the nanodots is because of (i) smoothing of dot surface along the beam direction due to unequal sputtering of different parts of dots (ii) re-deposition of adatoms and (iii) the ion induced surface diffusion. The sputtering yield is a function of $\text{Cos}^{-n}(\theta)$, where n is an integer, which differ from material to material [14, 21]. This indicates that sputtering increases with increasing angle of incidence. It falls down sharply at grazing incidences.

Considering the schematic in Fig. 4, at the oblique incidences, the ions hit the handout surface at different incident angles with respect to the respective surface

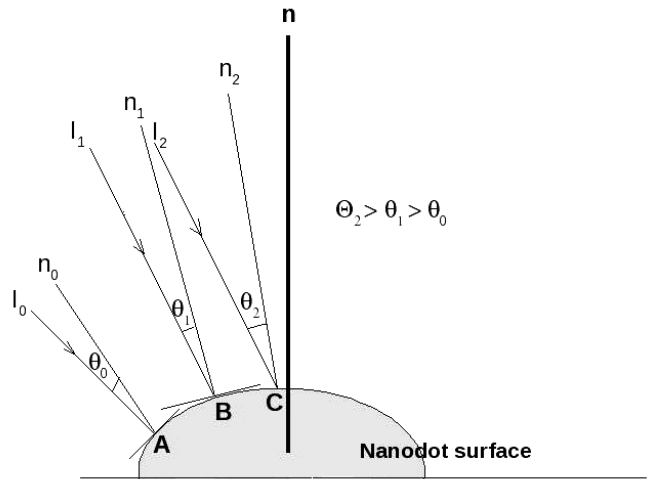


Fig. 4. Schematic of a nanodot surface, the incoming ions I_0, I_1 , and I_2 , at an angle of 30° with respect to flat surface normal n , making angles θ_0, θ_1 and θ_2 with surface normals n_0, n_1 and n_2 of the nanodot at points A, B and C respectively.

normal due to the surface curvature. As the angle, $\theta_2 > \theta_1 > \theta_0$, there will be more sputtering of the top part than the bottom of the dots, which results in the surface smoothing. Further, the sputtered atoms are re-deposited in the forward direction resulting in the elongation of dots along the beam direction [22]. The ion-induced surface diffusion too causes elongation of the surface structures. At oblique incidences, both the components of the forces contribute unequal energies in the two directions around the ion paths. There is a resultant driving force for surface diffusion to contribute causing the elongation of the nanostructures along the beam direction. This will be more prominent for 53° and 63° incidences. At $\theta_{\text{atom}} = 53^\circ$ and 63° , ripples are observed, with their wave vector perpendicular to the direction of the atom beam. The ripple orientation is in accordance with the one obtained for GaSb case studied by T. Alimers et al. [23]. The observed ripple wavelengths are ~ 55 nm and 60 nm respectively for 53° and 63° incidences. Finally, at 76° incidence, roughness of surface is almost equal to that of pristine sample. When the atoms are coming at grazing incidence, they interact less with the target surface due to lesser number of atoms reaching the surface. From our previous study [12], InP (100) was bombarded with 1.5 keV Ar atoms at different fluences varying from 4×10^{16} to 3.2×10^{17} atoms/cm², the angle of incidence was fixed at 45° with respect to the surface normal. The bombardment was carried out at room temperature at a pressure of 5×10^{-6} torr. The wavelength versus fluence graph is plotted as shown in Fig. 5. It is noted that wavelength, λ , depends on ion fluence, ϕ , as $\lambda \sim \phi^{0.36}$. This is contradictory to the linear BH equation, which predicts λ to be independent of the fluence. The wavelength observed in this case for 45° incidence angle is in accordance with this relation for the given fluence.

The graph between the angle of incidence and the wavelength of ripples obtained is plotted in Fig. 6 and it was found that the wavelength increases linearly with angle. This implies that as the angle is increased the wavelength also increases and the wavelength lies between 40 to 60

nm. Although, they not shown continuous ripple for incidence from 38 to 53°. BH theory is not sufficient to explain (i) the dependence of ripple wavelength on ion fluence and (ii) formation of nanodots on the surface. The dependence of wavelength on ion fluence and dot formation are explainable by non-linear Kuramoto-Sivashinsky equation due to incorporation of second order terms which were not included in the BH equation. KS equation explains the ion beam erosion under normal incidence which leads to formation of holes or dots on the surface depending upon the sign of the nonlinear parameter [24, 25]. Further understanding related to this theory is in progress with the help of numerical simulations.

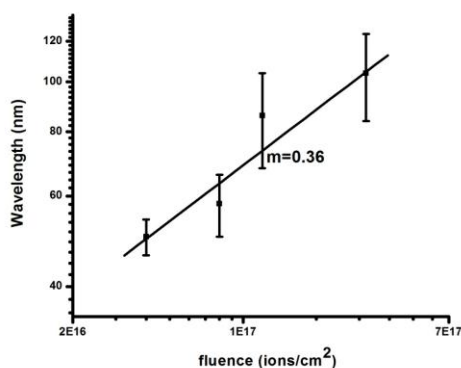


Fig. 5. Graph between average wavelengths of the nanoripples with ion fluence (extracted from our previous study).

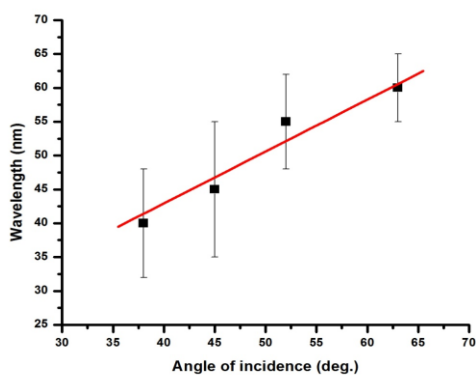


Fig. 6. Graph between angle of incidence and wavelength of ripples obtained.

Conclusion

In conclusion, it was demonstrated that low-energy Ar atom beam erosion could be used to produce different self-organized patterns on InP surface. The experimental results show distinct transitions between different patterns by varying the ion incidence angle. The nanodots of 32 to 100 nm diameter can be synthesized by tuning the angle of incidence. Also the ripple wavelength could be changed for 50 to 100 nm. Starting with normal ion incidence, nanoscale dots emerge on the surface of InP which transform into highly ordered nanodots for 13° incidence.

Further, nano ripples were observed, when the incidence angle is changed beyond 45°. The evolution of ripples from dots occurred at 23° where the dots start aligning and elongating in the direction of the beam. The rms roughness decreases with increase in incidence angle of the beam indicating the role of smoothing term. Further, simulation is required to explain the origin of these structures with variation in angle of incidence. These structures are formed on the InP surface due to interplay between the erosion and smoothing due to ion enhanced surface diffusion.

Acknowledgements

Authors would like to thank Department of Science and Technology, Govt. of India, for providing the SPM facility at IUAC, New Delhi. The author would also like to thank Dr P. Karmakar for his expert suggestion in this work. We also acknowledge the help of Mr R Abhilash during the bombardment.

References

- Kamins, T.I.; Williams, R.S. *Appl. Phys. Lett.* **1997**, *71*, 1201
- Facsko, S.; Kurz, H.; Dekorsy, T. *Phys. Rev. B* **2001**, *63*, 165329.
- Garcia, Javier Munoz; Gago, Raul; Vazquez, Luis; Sanchez Garcia, Jose Angel; Cuerno, R. *Phys. Rev. Lett.* **2010**, *104*, 026101
- Carter, G.; Vishnyakov, V. *Phys. Rev. B* **1996**, *17*, 647
- Facsko, S.; Dekorsy, T.; Koerd, C.; Trappe, C.; Kurz, H.; Vogt, A.; Hartnagel, H.L. *Science* **1999**, *285*, 1551
- Jiang, Z.X.; Alkemade P.F.A. *Appl. Phys. Lett.* **1998**, *73*, 315
- Erlebacher, J.; Aziz, M.J.; Chason, E.; Sinclair, M.B.; Floro, J.A. *Phys. Rev. Lett.* **1999**, *82*, 2330
- Bradley, R.M. & Harper, J.M.E. *J. Vac. Sci. Technol. A* **1988**, *6*, 2390
- Sung, M.M.; Lee, S.H.; Lee, S.M.; Marton, D.; Perry, S.S.; Rabalais, J.W. *Surf. Sci.* **1997**, *382*, 147
- Demagnet, C.M.; Sankar, K.V.; Malherbe, J.B. *Surf. Interface Anal.* **1996**, *24*, 503
- Tan, S.K.; Wee, A.T.S. *J. Vac. Sci. Technol. B* **2006**, *24*(3), 1444
- Sulania, I.; Tripathi, A.; Kabiraj, D.; Verma, S.; Avasthi, D.K. *J. Nanosci. Technol.* **2008**, *8*(8), 4163
- Sigmund, P. *J. Matter. Sci.* **1973**, *8*, 1545
- Barabasi, A.L.; Stanley, H.E. *Fractal Concepts in Surface Growth*, Camb. Univ. Press, **1995**.
- Frost, F.; Schindler, A.; Bigl, F. *Phys. Rev. Lett.* **2000**, *85*, 4118
- Kabiraj, D.; Abhilash, S.R.; Vanmarcke, L.; Cinausero, N.; Pivin, J.C.; Avasthi, D.K. *Nucl. Instrum. Methods in Phys. B* **2006**, *244*, 100
- Avasthi, D.K.; Mishra, Y.K.; Kabiraj, D.K.; Lalla, N.P.; Pivin, J.C. *Nanotechnology* **2007**, *18*, 125604
- Mishra, Y.K.; Mohapatra, S.; Avasthi, D.K.; Kabiraj, D.; Lalla, N.P.; Pivin, J.C.; Sharma, H.; Kar, R.; Singh, N. *Nanotechnology* **2007**, *18*, 345606
- Mishra, Y.K.; Mohapatra, S.; Singhal, R.; Avasthi, D.K. *Appl. Phys. Lett.* **2008**, *92*, 043107
- Mohapatra, S.; Mishra, Y.K.; Avasthi, D.K.; Kabiraj, D.; Ghatak, G.; Varma, S. *Appl. Phys. Lett.* **2008**, *92*, 103105
- Chini, T.K.; Bhattacharya, S.R.; Basu, A.D.; Biersack, J.P. *Radiation effects and defects in solids* **1994**, *127*, 349.
- Castro, M.; Cuerno, Rudolf; Vazquez, Luis & Gago, Raul; *Phys. Rev. Lett.* **2005**, *94*, 016102
- Alimers, T.; Donath, M.; Rangelov, G. *J. Vac. Sci. Technol. B* **2006**, *24*(2), 582.
- Ziberi, B.; Frost, F.; Rauschenbach, B. *Appl. Phys. Lett.* **2006**, *88*, 173115.
- Ziberi, B.; Frost, F.; Hoche, T. Rauschenbach, B. *Phys. Rev. B* **2005**, *72*, 235310.